Paper Number: **101**

Title: **Applying a Stiffened Stitched Concept to Shear-Loaded Structure**

Author: Dawn Jegley

ABSTRACT

NASA and The Boeing Company have worked to develop new low-cost, light-weight composite structures for aircraft. A stitched carbon-epoxy material system was developed to reduce the weight and cost of transport aircraft structure, first in the NASA Advanced Composites Technology (ACT) Program in the 1990's and now in the Environmentally Responsible Aviation (ERA) Project. By stitching through the thickness of a dry carbon fiber material prior to cure, the need for mechanical fasteners is almost eliminated. Stitching also provides the benefit of reducing or eliminating delaminations, including those between stiffener flanges and skin. The stitched panel concept used in the ACT program used simple blade-stiffeners as stringers, caps, and clips. Today, the Pultruded Rod Stitched Efficient Unitized Structure (PRSEUS) concept is being developed for application to advanced vehicle configurations. PRSEUS provides additional weight savings through the use of a stiffener with a thin web and a unidirectional carbon rod at the top of the web which provides structurally efficient stiffening. Comparisons between stitched and unstitched structure and between blade-stiffened and rod-stiffened structure are presented focusing on a panel loaded in shear. Shear loading is representative of spar loading in wing structures.

INTRODUCTION

NASA and The Boeing Company have worked to develop new low-cost, light-weight composite structures for aircraft. As a consequence of this effort, a stitched carbon-epoxy material system was developed with the potential for reducing the weight and cost of transport aircraft wing structure in the NASA Advanced Composites Technology (ACT) Program in the 1990's [1]. By stitching through the thickness of a dry carbon fiber material prior to cure, the labor associated with panel fabrication and assembly can be significantly reduced and the need for

Dawn C. Jegley, NASA Langley Research Center, Mail Stop 190 Hampton Virginia 23681, U.S.A.

mechanical fasteners is almost eliminated. Stitching provides the benefit of reducing or eliminating delaminations, including those between stiffener flanges and skin. Stitching reduces part count, and therefore, cost of the structure.

The technology developed in the NASA ACT Program used simple blade-stiffeners as stringers and spar caps. Stitching allows for the elimination of fasteners in panel acreage, and its damage arresting capabilities make it suitable for wing structure. Today, in NASA's Environmentally Responsible Aviation Project (ERA), NASA and Boeing are advancing stitching technology by developing a Pultruded Rod Stitched Efficient Unitized Structure (PRSEUS) concept [2,3] for application to advanced vehicle configurations. An example of an advanced vehicle configuration is high-aspect ratio wings which will improve aerodynamic performance. Both the stitched blade-stiffened and the PRSEUS concept can be applied to high-aspect ratio wings.

The stitching approach consists of carbon-epoxy panels fabricated from dry components, stitched, and then infused with resin. In both blade-stiffened and PRSEUS concepts, skins, flanges, and stiffeners contain layers of graphite material forms using Hercules, Inc. AS4 or similar fibers that are prekitted in multi-ply stacks. Several stacks of the prekitted material are used to build up the desired thickness and configuration. The prekitted stacks have a [44/44/12] percent distribution of 0-, $\pm$45-, and 90-degree plies. Nominal stack thickness was 0.055 inches for blade-stiffened panels and 0.052 inches for PRSEUS panels. Any number of stacks can be assembled to obtain the desired thickness. All stiffener flanges are stitched to the skin and no mechanical fasteners are used for joining. A Kevlar stitching thread is used for the blade-stiffened panel and a Vectran stitching thread is used for the PRSEUS panels. A sketch of the blade-stiffened cross section is shown in Figure 1.

A PRSEUS structure includes a stiffener consisting of a thin web and a unidirectional carbon rod at the top of the web to provide structurally efficient stiffening in one direction while foam-filled frames are positioned perpendicular to the rod-stiffeners to provide stiffening in the other direction. A sketch of the cross section of a PRSEUS rod-stiffened stringer is shown in Figure 2. The rods are Toray unidirectional T800 fiber with a 3900-2B resin or a similar material. Note that the number of stacks around the rod (overwrap stacks) is always half the number of web stacks. Similarly, the number of stacks in the flange is always half the number of stacks in the stringer web. Tear straps made of one or more stacks can be added between the skin and the flange if extra reinforcement is needed.

Most evaluations of PRESUS to date have focused on axial or pressure loading. Applying rod-stiffeners and stitching to shear-loaded structure is the subject of this paper. The weight benefit potential by using stitching and rod-stiffeners is considered analytically herein. First, an unstiffened unstitched panel is compared to a stitched unstiffened panel with the same geometry and boundary conditions. Then, a blade-stiffened panel with mechanically fastened stiffeners is compared to a rod-stiffened panel without mechanical fastening. The objective of this paper is to demonstrate weight savings that could be achieved by using stitching and rod-stiffeners for shear-loaded structure such as wing spars.

Experimental and analytical displacements and strains for an unstitched unstiffened panel and a blade-stiffened panel are presented first to establish the accuracy of the analytical methodology. Stitched and rod-stiffened panels with the

same overall geometry are then examined to determine how much weight could be saved by switching from mechanically fastened blade-stiffened structure to a stitched rod-stiffened concept.

EXPERIMENTAL PANEL DESCRIPTIONS

Two panels are considered based on test data previously acquired. Test data for seven 8-ply shear panels made of AS4-3502 tape are presented in reference 4. The unstiffened quasi-isotropic panel for which extensive data is presented in reference 4 is used as a baseline panel herein. A photograph of the unstiffened panel test article is shown in Figure 3. This panel had no stitching. The panel test section is 12 in. by 12 in. A more detailed description of the unstiffened baseline panel is presented in reference 4.

The second baseline panel was a blade-stiffened panel consisting of two blade-stiffeners mechanically fastened to the skin. Blades were 2.25 inches tall and spaced 8 inches apart. Stiffener flanges were 3.2 inches wide. The skin and stringers were stitched and cured independently and then the flanges were mechanically fastened to the skin. Stringer blades contained 8 stacks, stringer flanges contained 4 stacks and the skin contained 4 stacks. A photograph of the blade-stiffened test article geometry is shown in Figure 4. A 6-inch-diameter circular cutout in the center of the stiffened panel was added to represent an access hole in a typical spar segment. Note that since the stiffeners were mechanically attached to the skin, this panel is not representative of fully stitched structure.

The calculated weight of the baseline unstiffened panel is 0.33 lb. The calculated weight of the baseline stiffened panel is 8.2 lb plus fastener weight. For both baseline types, metallic doublers were bonded to the edges of the panel to assist in load introduction and are not included in panel weight. Panel dimensions for the unstiffened and stiffened test articles are shown in Figures 3 and 5, respectively.

TEST PROCEDURE AND INSTRUMENTATION

The test panels were loaded in shear at the NASA Langley Research Center. For the unstiffened panel, 24 strain gages, one displacement transducer measuring displacement at the center of the panel and one longitudinal displacement transducer were used to monitor panel behavior. For the stiffened panel, 22 strain gages, four lateral displacement transducers and one longitudinal displacement transducer were used to monitor panel behavior. Each test article was loaded by pulling on the fixture at one corner at a rate of 500 lb/min for the unstiffened panels and 15,000 lb/min for the stiffened panel. In each case the diagonally opposite corner was held in place. Buckling and failure behavior were noted for all panels.

ANALYSIS APPROACH

Finite element analyses of the unstiffened and the blade-stiffened test articles were conducted to compare analytical results to the test data. The analyses were conducted using the finite element code STAGS [5]. All composite parts of the test articles were modeled as 4-node quadrilateral shell elements (STAGS element E410). Edge supports and load introduction hardware are represented by beam elements in the unstiffened test article model and shell elements in the stiffened test article model. Nominal properties for the composite plies in the shell elements for the unstiffened test article model and for the stack of material for the stiffened test article model are shown in Table I.

TABLE I. NOMINAL MATERIAL PROPERTIES

Property	Unstiffened panel ply	Stitched Stack	Rod	Steel
Longitudinal modulus, Msi	18.5	9.23	18.0	28.0
Transverse modulus, Msi	1.67	4.66	1.0	28.0
Shear modulus, Msi	.87	2.26	6.0	10.8
Poisson's ratio	.30	0.397	0.2	.3
Thickness, in.	0.0052	0.055*	NA	1.75
Density (lb/in^3)	0.055	0.057	0.057	.29

*Stack is [44/44/12] percent 0/±45/90; 0.055 inches thick for blade-stiffened, 0.052 inches thick for PRSEUS

Element size was between 0.25 and 0.5 inches per side for all models. The models for the unstiffened and stiffened test articles are shown in Figures 6a and 6b, respectively. For the unstiffened panel, a tensile load was applied at one corner of the panel while no motion was permitted at the diagonally opposite corner. In the stiffened panel model, rigid links were used to represent fasteners connecting skin nodes to flange nodes at the locations where fasteners were used in the blade-stiffened test article. In the stiffened panel model, load introduction hardware including the 2.75-in.-wide, 1.75-in.-thick steel plates which are shown in figures 4 and 5 were included along the panel edges in the model. Properties of the load introduction hardware are shown in Table I. Multi-point constraints were used to connect the load introduction plates to each other and a tensile load was applied at one corner of the test article assembly, as shown in Figure 6. No motion was permitted at the comparable location of the diagonally opposite corner.

Out-of-plane motion was restrained along all edges. The unstiffened panel model contained 2700 elements and 15,606 degrees of freedom. The stiffened panel model contained 24,997 elements and 157,177 degrees of freedom. The analysis accounted for geometric nonlinearities but not plasticity. For the unstiffened panel, a buckling load was calculated based on a linear prebuckling stress state. Then, an assumed imperfection in the shape of the buckling mode corresponding to the minimum buckling load was input. An imperfection mode with an amplitude of approximately 10 percent of the panel thickness was input to trigger nonlinear behavior for loads greater than the buckling load. This trigger was not necessary

for the stiffened panel. Geometrically nonlinear analysis with and without damage progression were conducted.

A discussion of damage progression analysis is presented for unstitched and stitched structure in references 6 and 7, respectively. Failure properties for unstitched and stitched plies are given in Table II [6,8]. In the damage progression approach used herein, the STAGS "linear orthotropic elastic brittle material" is used to represent the composite elements. A maximum stress criteria is used wherein the calculated in-plane stress is compared to the failure stress in each point in each composite element to determine if a matrix or fiber failure has occurred. Tension, compression, and shear are considered independently. Damage is tracked ply-by-ply within each element. Each ply in the damage progression model is evaluated individually at three integration points through the thickness. The material degradation model used in the present analysis assumes complete failure at the location where a stress allowable is exceeded. Failure results are shown in terms of the percentage of "material points" within each element which have failed. The number of material points in an element is dependent upon the number of surface-integration points, the number of layers in the laminate, and the number of through-the-thickness integration points per layer.[6]

After demonstration that the finite element model of the test article produced results that agreed with the test data, stitched properties were substituted for unstitched properties in the damage progression analysis of the unstiffened panel model.

In the unstiffened panel, few opportunities for weight reduction are available. Damage progression analysis predictions are compared for the baseline panel and a quasi-isotropic skin of stitched plies. While this is not a standard stitched stack, such a panel could be fabricated and represents a direct comparison with the test article.

TABLE II. FAILURE PROPERTIES

Property	Tape AS4-3501 ply (ksi)	Stitched AS4-3501-6 ply (ksi)
Tensile failure longitudinal stress, 0-degree ply	233	257
Tensile failure longitudinal stress, +45 and -45-degree plies,		231
Tensile failure longitudinal stress, 90-degree ply,		213
Compressive failure longitudinal stress, all plies	210	175
Tensile failure transverse stress, all plies	14.7	5.88
Compressive failure transverse stress, all plies	28.7	36.5
Shear failure stress, all plies	29.7	20.6

The same approach is used to analyze the stiffened panel that was used to analyze the unstiffened panel. However, in the stiffened panel model, blade stiffeners were replaced with rod stiffeners. Additionally, the fastener elements

were removed and skin and flange elements combined. In fabricated rod-stiffened panels, the pultruded rods are typically shaped like a teardrop but for simplification, a circular cross-section pultruded rod was used in this study. Beam elements were used to model the combination of the pultruded rod and the surrounding overwrap stack(s) of material. The rod-stiffened model contained 23,541 elements, and 17,526 degrees of freedom. Rod properties are shown in Table I [2]. The same methodology for modeling stitched structures is used in references 9-11 as used herein, namely that no solid elements are used and that the combination of the rod and overwrap are defined as a beam element. Skin and flange regions which are stitched and cocured are treated as one unit and no delaminations are permitted. Since rod failure has not been the initial failure in any PRSEUS structure tested to date, rod failure is not included in this analysis. Nonlinear damage progression analysis was performed for the PRSEUS structure.

To explore possible weight reductions in the rod-stiffened panel model, rod diameter, flange width, rod-stringer height, web thickness, skin thicknesses, and tear strap thickness were varied. Nonlinear analysis of each promising design was performed to determine if rod-stiffened panels could be designed to be lighter than the blade-stiffened panel while supporting a failure load level equal to or greater than that of the test article. Buckling behavior, strain levels, and damage progression were evaluated.

RESULTS AND DISCUSSION

In this section experimental and analytical results for an unstiffened unstitched test article are presented. Displacements, strains, and failures are discussed. Then analytical results for the equivalent stitched panel are presented. Subsequently analytical and experimental results for the stiffened test article with mechanical fasteners are presented, followed by the analytical results for a stiffened panel in which the stiffeners are stitched to the panel skin.

Unstiffened panels

The experimental results for the $[\pm 45/0/90]_s$ panel presented in reference 4 is used herein to confirm that the analytical approach gives accurate results. Load versus out-of-plane deformation and strain are shown in Figures 7 and 8, respectively. Experimental results taken from reference 4 are shown as solid lines. Analytical results are shown as long dashed lines for analysis without damage progression and short dashed lines for analysis with damage progression. Out-of-plane deformation is normalized by panel thickness and load is normalized by the buckling load, in keeping with the method of presenting results in reference 4. Back-to-back strain gage results at the center of the panel for axial and lateral strains are labeled A and B, respectively. A and B each represent a back–to-back pair so strains on the top and bottom surfaces are shown. Displacement and strain results for the experiment are in good agreement with the analytical results.

The experimental failure load was 25.5 kips. Damage progression analysis predicted failure initiation at 25.6 kips and final failure at 28.1 kips. Initial damage developed in both -45^o plies in matrix tension in 902 elements near the center of the

panel in a region running between the clamped point and the loaded point. The number of elements suffering matrix damage in the -45^{o} plies continud to grow as load was increased. The damaged elements at a load of 28.1 kips are shown in Figure 9a. By a load of 28.1 kips, 1288 elements have suffered some damage and damage is not limited to the -45^{o} plies. In the figure, the percentage of "material points" within each element which has failed is shown based on the colored scale. The failure is limited to the center region of the panel. The failure region is similar to the region seen in the test article [4]. The combination of displacement and strain gage comparisons and the damaged region imply that the analytical model is adequate to predict specimen behavior.

Substituting stitched material properties in the analytical model results in similar strains and displacements with failure initiating at a load of 24.0 kips and complete failure at 26.5 kips. Initial failures occur in both -45^{o} plies in matrix tension in 302 elements near the center of the panel in a region running between the clamped point and the loaded point. By a load of 26.5 kips, 2162 elements have sustained damage and the damage mechanisms include in-plane shear and fiber compression and additional plies have suffered some damage. The damaged elements at the maximum loading of the panel are shown in Figure 9b and demonstrate a more concentrated failure region since differences in material properties, including failure properties, change which plies and which elements sustain damage and change the load redistribution. Because of the slight waviness in the fibers induced by the addition of stitches, in general, in-plane properties are slightly less than the properties of a laminate with the same stacking sequence but not stitched. Analyses and test article behavior indicate that the panel would support load far into the post-buckling region. The weight difference between these two panels is negligible and the failure loads are comparable.

Stiffened panels

Experimental and analytical surface strains at the edge of the cutout for the blade-stiffened test article are shown in Figures 10 and 11. Experimental results are shown as solid lines. Analytical results are shown dashed lines for analysis with damage progression. For simplicity, results without damage progression are not included. Vertical strain gage locations are labeled A and B. Lateral strain gage locations are labeled C and D. One pair of back-to-back strain gages (identified as top and bottom surfaces in the figure) is located at each of these four points. The vertical strain gages measure tensile strains throughout the loading. The dashed line for points A and B only go up to a load of 77 kips because damage initiates in these elements and surface strains can no longer be calculated. Lateral back-to-back strain gages initially measure a compressive load. However, the back-to-back gages show slope changes representative of buckling at a load of approximately 55 kips for both experiment and analysis. Results for the experimentally measured strains are in good agreement with the analytical results.

Full field out-of-plane displacement and skin surface shear strains are shown in Figure 12 and 13, respectively, at a load of 110 kips. Buckling behavior and strain concentrations at the hole edges are shown. Damage progression analysis indicates that damage would initiate at 62 kips and the maximum load would be 135 kips. Analysis indicates that initial failures occur in all -45^{o} plies in the skin in matrix

tension in 32 elements near the edge of the hole. The number of elements suffering matrix damage in the -45° plies continues to grow as load is increased. By the load of 135 kips, all plies have sustained damage and 3892 elements are partially failed. At the edge of hole, damage mechanisms of fiber tensile failures and fiber compressive failures have occurred.

The experimental failure load was 110 kips. A photograph of the failed panel is shown in Figure 14. The failure can be seen at the edge of the hole. The test article failed through the hole edge at location A in the strain plots. Damage can be seen locally at the hole edge and damage can be seen to follow a stitch line away from the hole edge to the stiffener flange. The location of the failure is consistent with the analytical results except that the analysis predicts failure in both corners A and B. Since typically there are small differences in hardware causing one location to fail before a nominally identical location, followed by additional damage from the initial failure location, this difference between failure prediction and experimental behavior is not surprising. Minor imperfections such as unevenness at the hole edge, slight initial geometric imperfections, or minor manufacturing defects that could have been present at the edge of the hole to trigger one location rather than another are not considered in the analysis. Failing elements, as indicated by the analysis, at a load of 110 kips and 135 kips are shown in Figure 15a and b, respectively. The colored scale represents the percentage of material points in each element that has failed. The failure moves outward from the hole edges. Flange elements do not fail in the analysis.

In the test article, after final failure, minor damage can be seen around a few of the fastener holes. Since the fastener holes were not included in the analysis, failures at the fastener holes could not be predicted by the analysis. The combination of strain gage comparisons and damaged region imply that the analytical model is adequate to predict specimen behavior.

Rod-stiffened panels with the same overall geometry are then evaluated analytically. Skin thickness, flange thickness, web thickness, rod diameter, stringer height were varied based on a PRSEUS design. Analysis indicates that adding a rod to the top of the blade does not result in a lighter design. In fact, the only difference between the blade-stiffened test article and an optimal PRSEUS design is assuming the flanges and skin are bonded/stitched instead of mechanically fastened and halving the blade and flange thickness. Damage progression analysis indicates damage will initiate at 68 kips and failure will occur at 135 kips.

Initial failures occur in all -45° plies in the skin in matrix tension in 86 elements near the edge of the hole. The number of elements suffering matrix damage in the -45° plies continues to grow as load is increased. By the load of 110 kips, more plies and more elements have damage. Matrix tension failure is still the predominant mode, however a few elements at the hole edge have sustained fiber compression failures. A total of 2929 elements have sustained some damage by 110 kips. Full field out-of-plane displacement and skin surface shear strains are shown in Figure 16 and 17, respectively, at a load of 110 kips. Buckling behavior and strain concentrations at the hole edges are shown. Failing elements, as indicated by the analysis, at a load of 110 kips and 135 kips are shown in Figure 18a and b, respectively. By the load of 135 kips, all plies have sustained damage and 3771 elements are partially failed. At the edge of hole, in-plane shear, matrix compression, and fiber compression failures have also developed. The colored

scale represents the percentage of material points in each element that has failed. The failure moves outward from the hole edges..

The fully stitched panel with changes in thickness results in approximately a 9% reduction in weight with no reduction in load carrying ability. This 9% reduction does not take into account the weight of the fasteners since the original panel model weight did not account for the fastener weight.

CONCLUDING REMARKS

Wing spars are an example of panels typically designed to support shear loading. Unstiffened and stiffened shear-loaded panels were examined. Thin stiffened shear-loaded panels offer opportunities for weight savings compared to conventional design by stitching the stiffeners to the skin rather than using mechanical fasteners.

REFERENCES

1. Karal, M. 2001. "AST Composite Wing Study – Executive Summary," NASA CR-2001-210650.
2. Velicki, A. 2009. "Damage Arresting Composites for Shaped Vehicles," NASA CR-2009-215932.
3. Jegley, D. and A. Velicki, 2013. "Status of Advanced Stitched Unitized Aircraft Structures," presented at the 51st AIAA Aerospace Sciences Meeting, January 7-10, 2013.
4. Rouse, M. 1985. "Postbuckling of Flat Unstiffened Graphite-Epoxy Plate Loaded in Shear," Thesis for George Washington University,Washington D.C.
5. Rankin, C. C., W. A. Loden, F. A. Brogan, and H. D. Cabiness. 2007. "STAGS Users Manual," Rhombus Consultants Group, Inc., Palo Alto, CA 94303.
6. Knight, N. and Rankin, C. 2006. "STAGS Example Problems Manual," NASA CR-2006-214281.
7. Jegley, D. 2005. "Structural Efficiency of Stitched Composite Panels with Stiffener Crippling," *J. of Aircraft,* 42(5):1273-1280.
8. McGowan, D., C. Davila, and D. Ambur. 2001. "Damage Progression in Buckle-Resistant Notched Composite Plates Loaded in Uniaxial Compression," presented at the 42nd AIAA Structures, Structural Dynamics, and Materials Conference, April 2001.
9. Jegley, D. 2011. "The Influence Of Restraint Systems on Panel Behavior," presented at Society of Experimental Mechanics Conference, June 2011.
10. Jegley, D. 2011. "Structural Efficiency and Behavior of Pristine and Notched Stitched Structure," presented at the SAMPE Fall Technical Conference, October 2011.
11. Jegley, D. 2013. "Behavior of Frame-Stiffened Composite Panels with Damage," Presented at the 54th AIAA Structures, Structural Dynamics, and Materials Conference, April 2013.

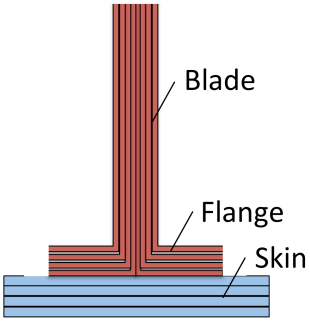

Figure 1. Blade-stringer cross section.

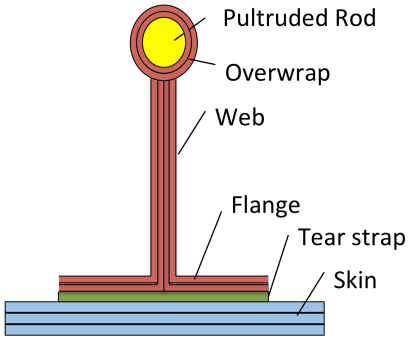

Figure 2. Rod-stiffener cross section.

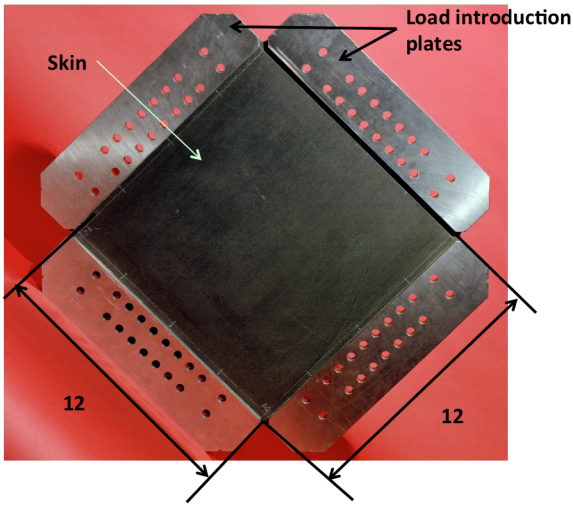

Figure 3. Unstiffened panel geometry. Dimensions are in inches

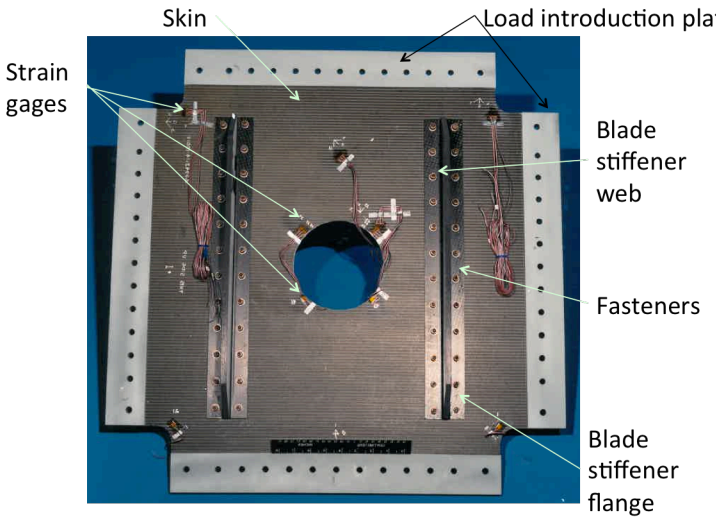

Figure 4. Stiffened panel geometry.

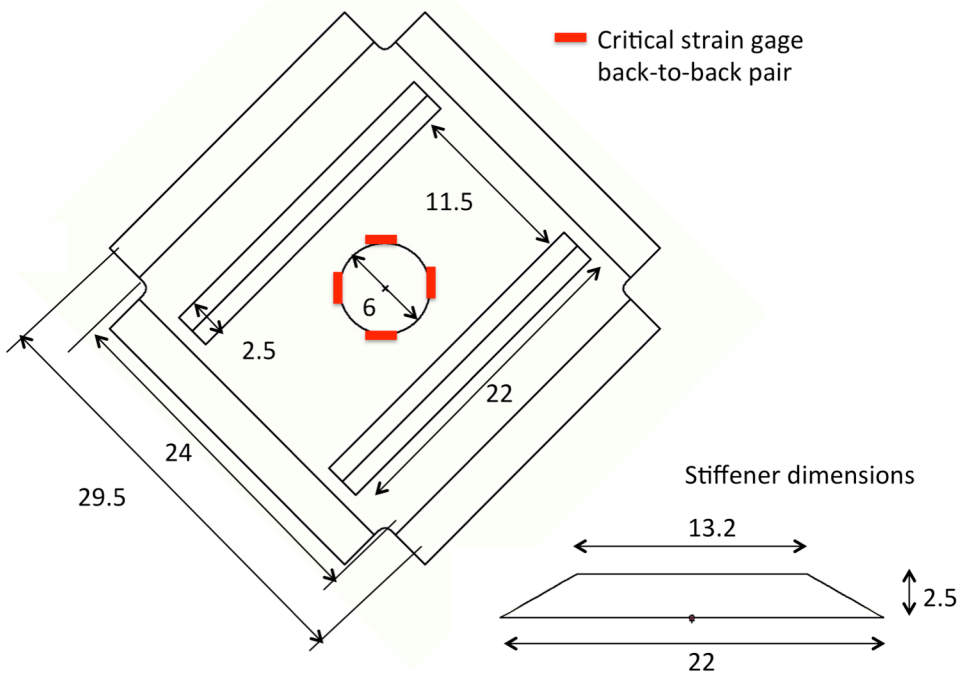

Figure 5. Stiffened panel geometry. Dimensions are in inches.

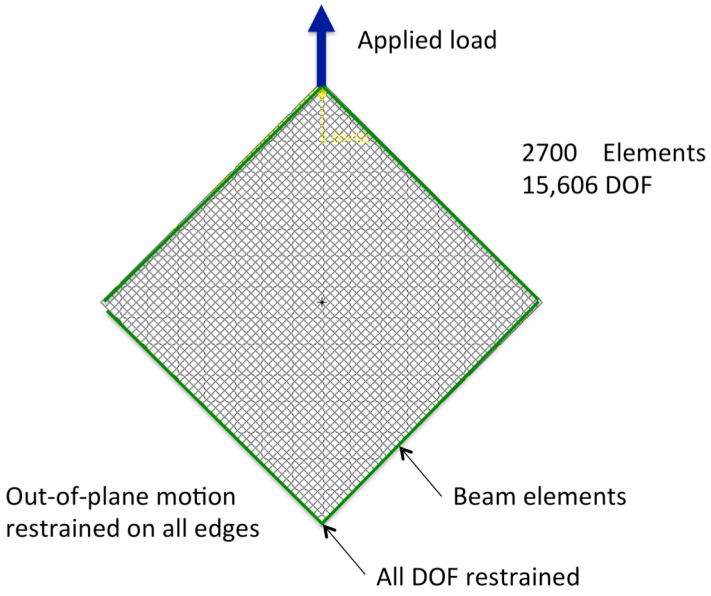

a) Unstiffened test article.

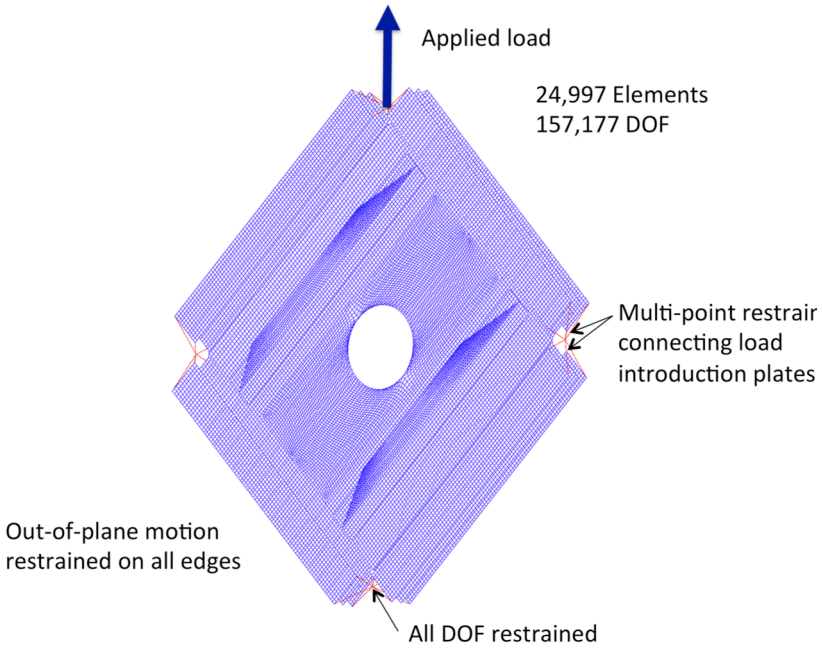

b) Blade-stiffened test article.

Figure 6. Finite element models

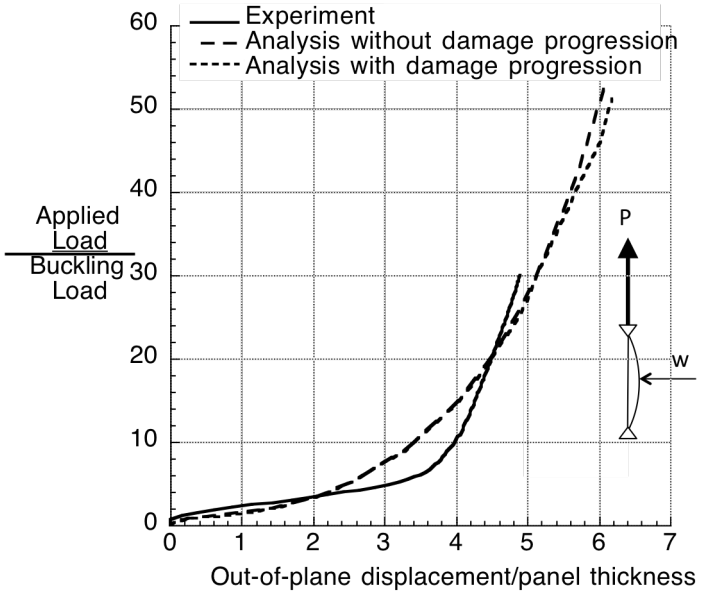

Figure 7. Out-of-plane deformation of unstitched unstiffened test article.

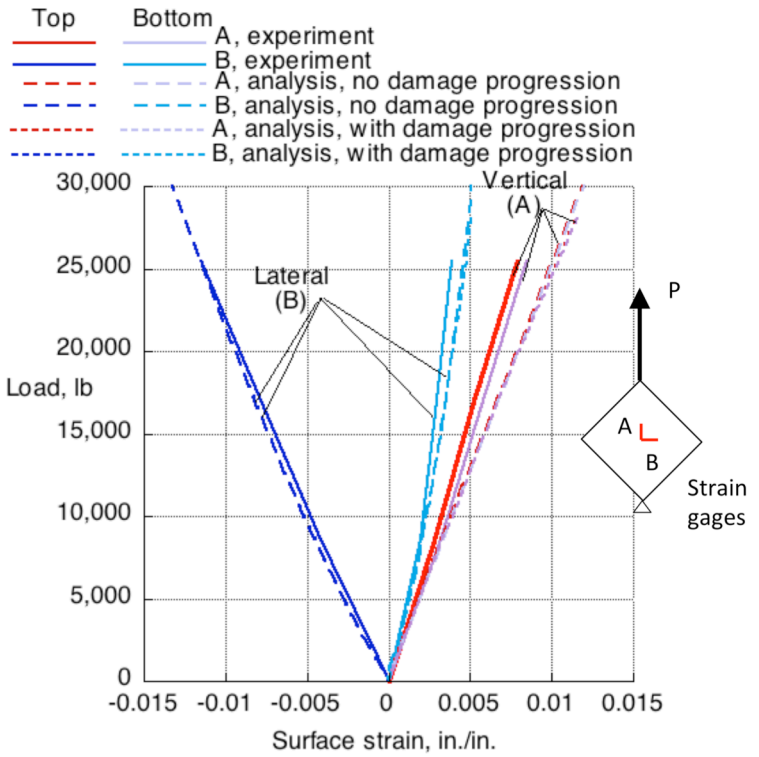

Figure 8. Surface strain in unstitched unstiffened test article.

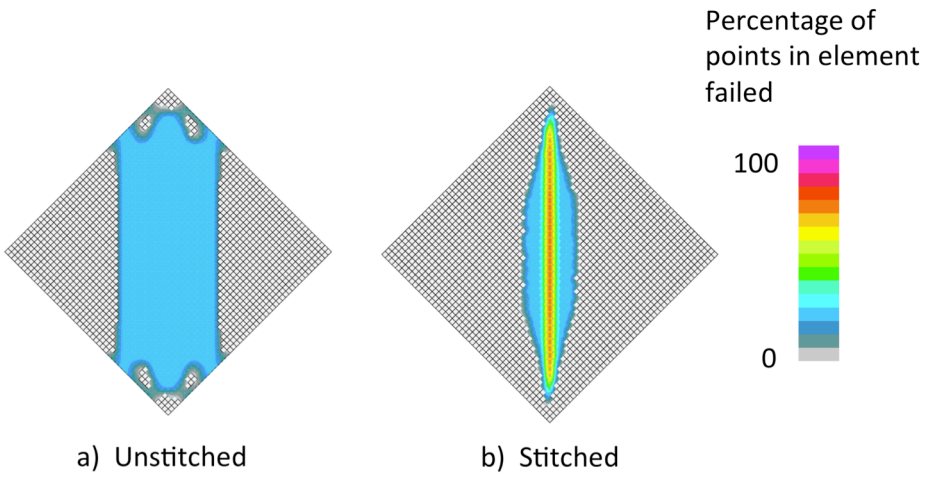

Figure 9. Damage in unstiffened panel at maximum load.

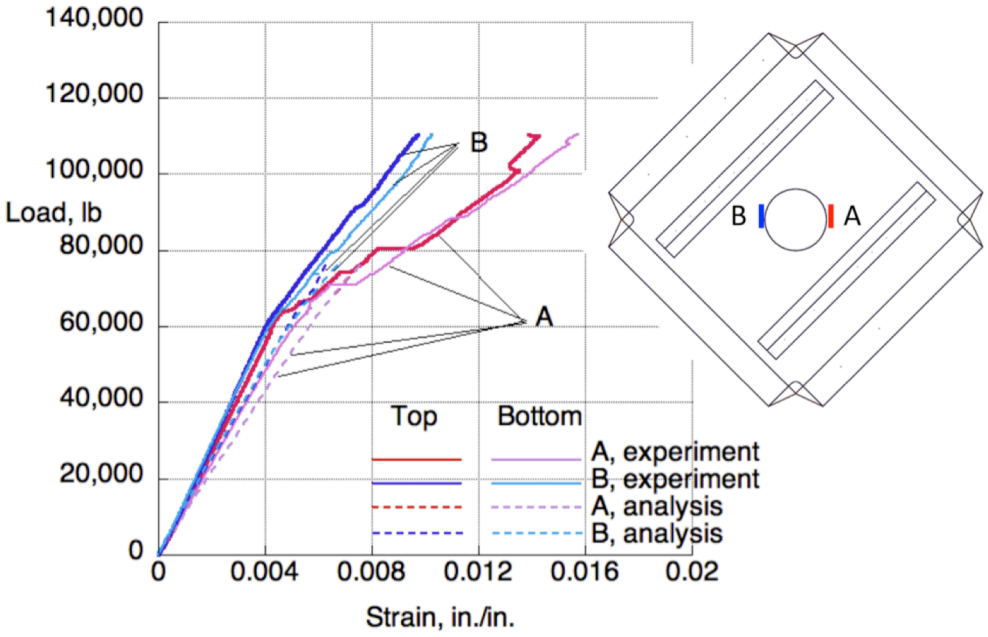

Figure 10. Vertical surface strain at cutout edge of stiffened test article.

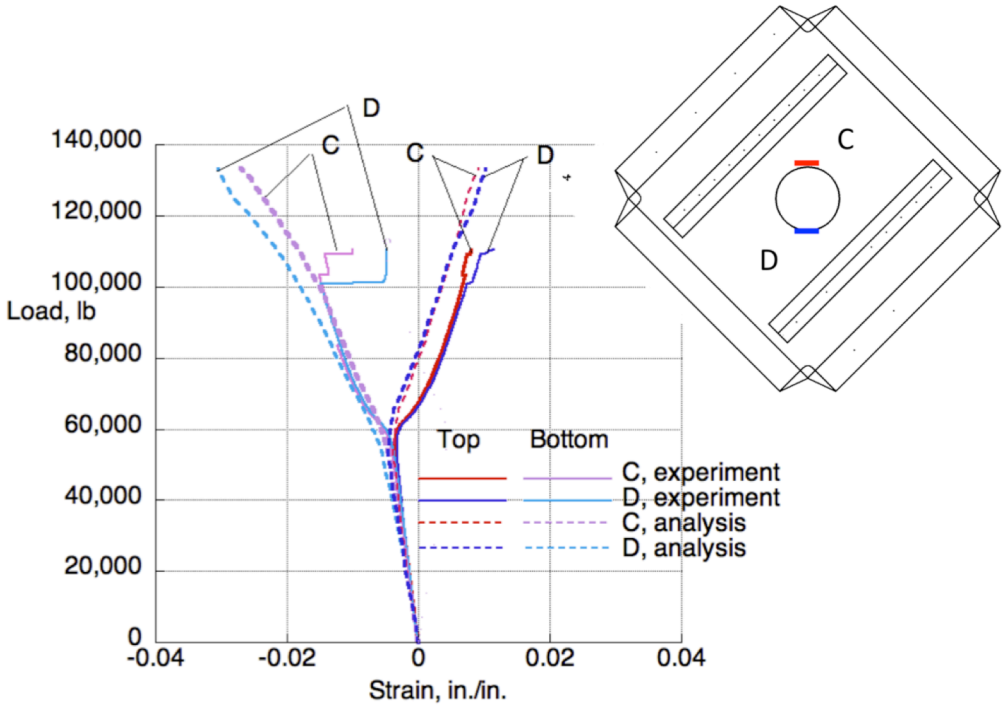

Figure 11. Lateral surface strain at cutout edge of stiffened test article.

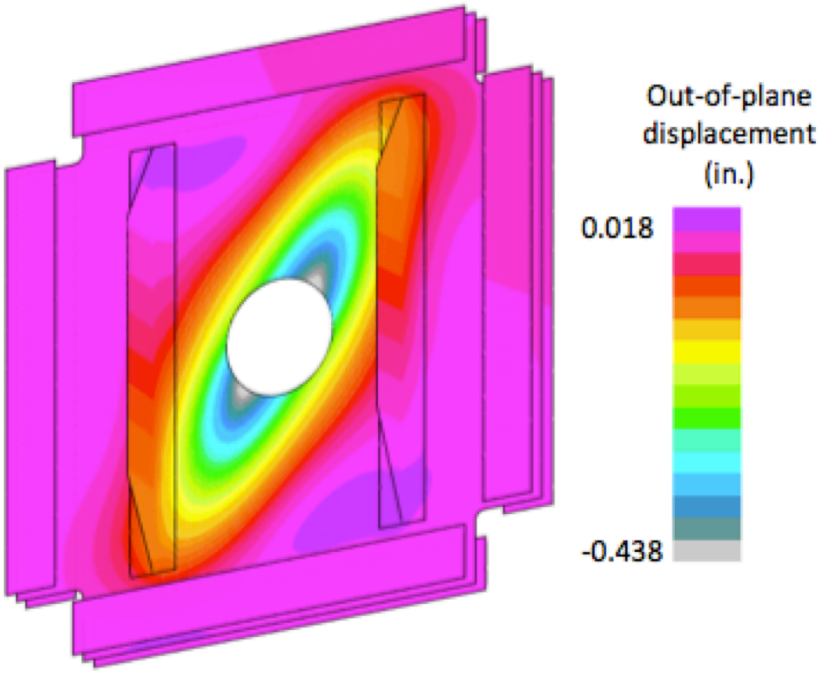

Figure 12. Predicted out-of-plane displacement at 110 kips for stiffened test article.

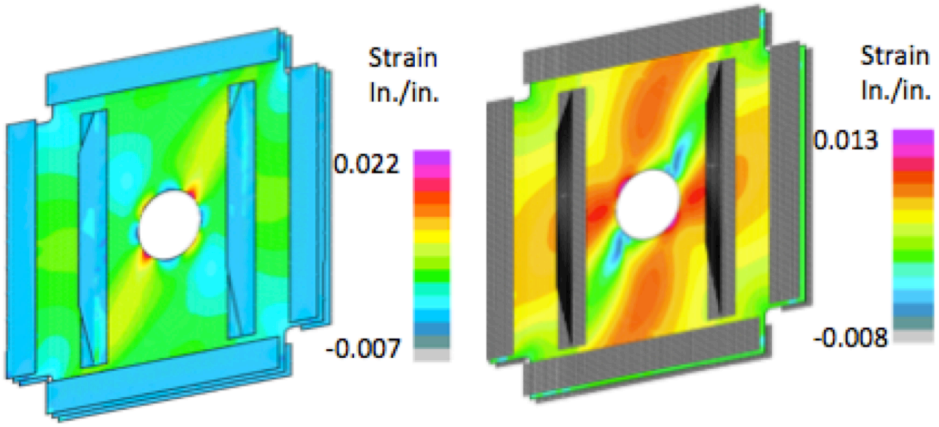

a) Bottom surface b) Top surface

Figure 13. Predicted surface shear strain at 110 kips for stiffened test article.

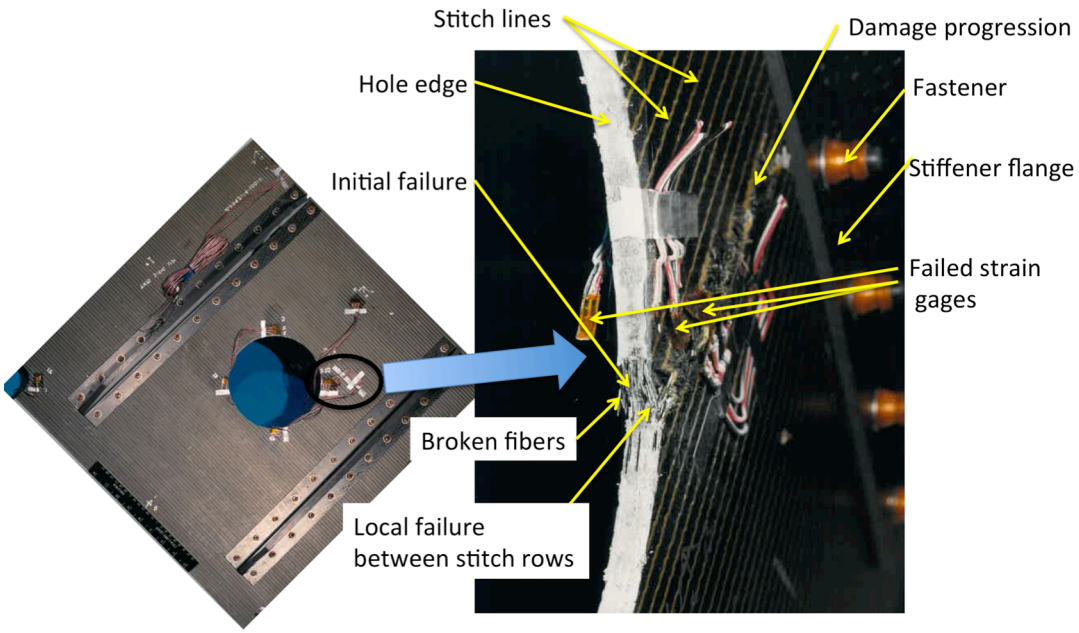

Figure 14. Failure of stiffened panel.

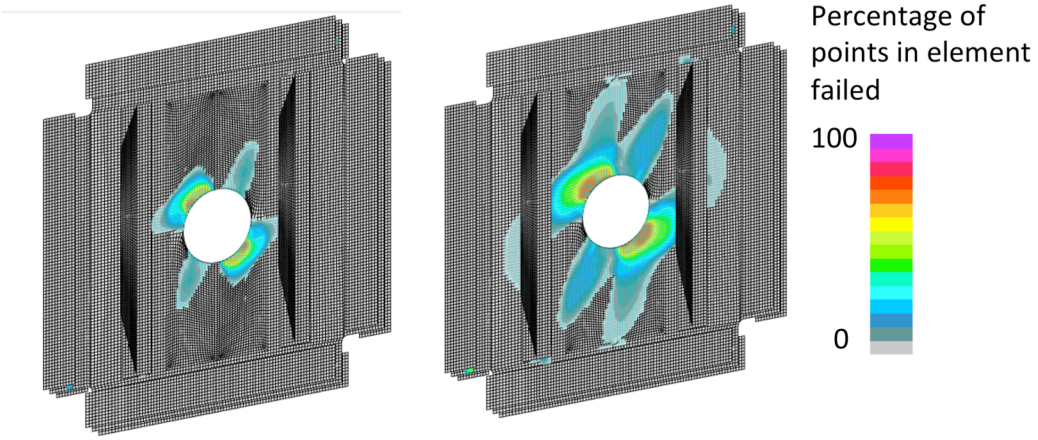

a) 110 kips b) 135 kips

Figure 15. Damaged elements in the stiffened test article analysis.

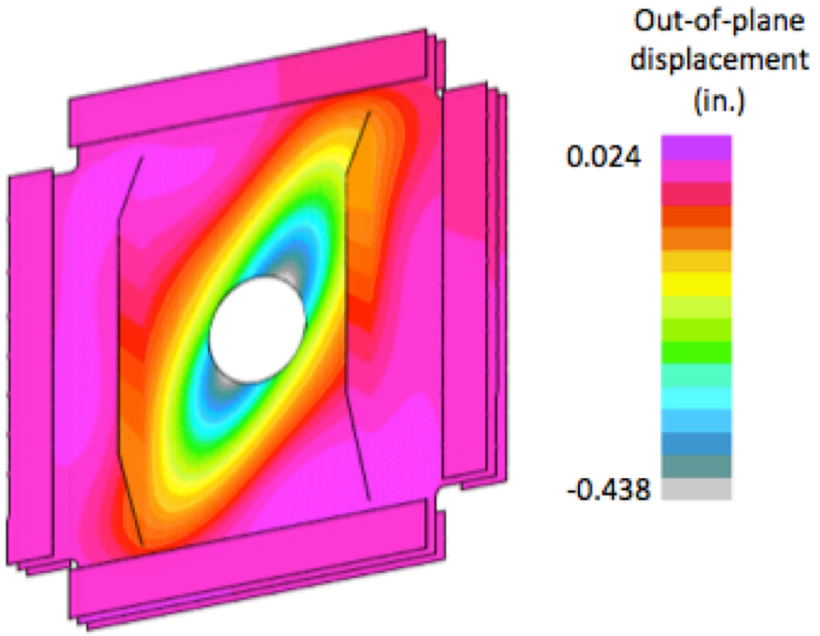

Figure 16 Predicted out-of-plane displacement at 110 kips for stiffened PRSEUS panel.

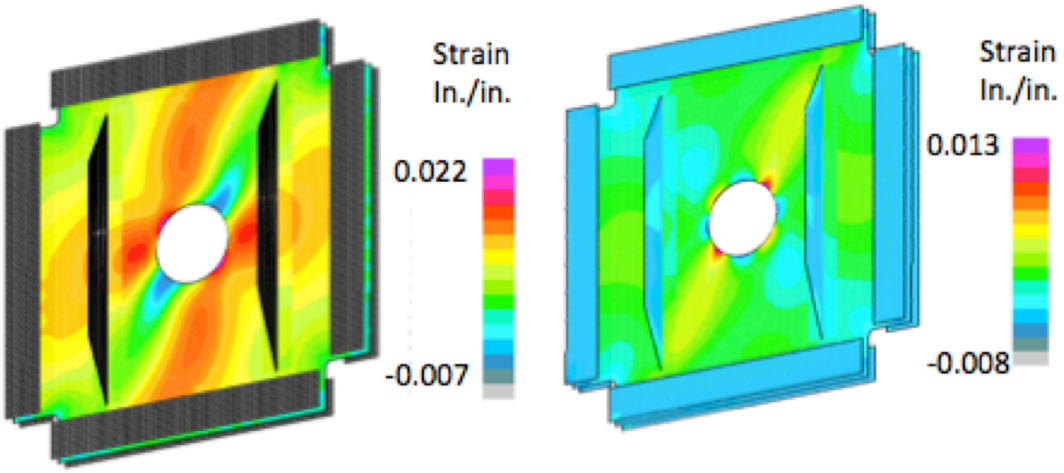

a) Bottom surface b) Top surface

Figure 17. Predicted surface shear strain at 110 kips for stiffened PRSEUS panel.

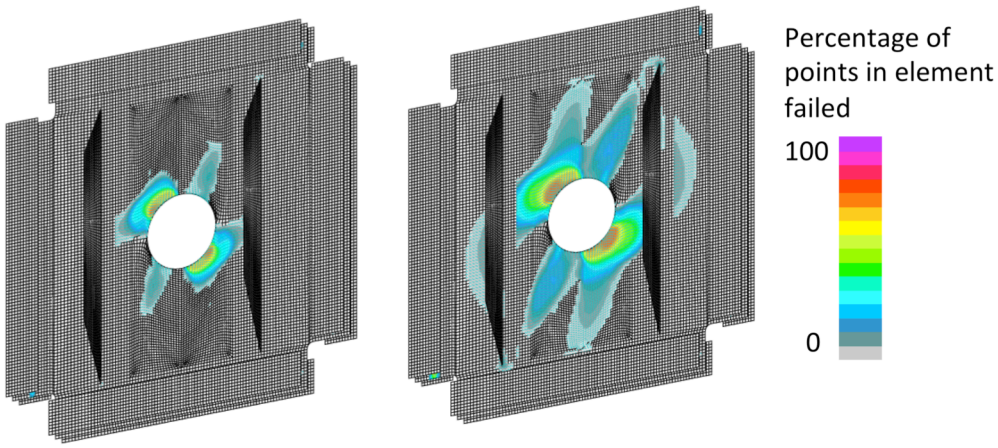

a) 110 kips b) 135 kips

Figure 18. Damaged elements in the stiffened test article analysis.